SNR研究における
CTAと他波長との連携

Yutaka Ohira Aoyama Gakuin University

Contents

- Cosmic rays and Supernova remnants
- Spectral index of accelerated particles
- Observations of SNRs
- Summary

Galactic cosmic ray

SNRs are though to be the origin of the Galactic CR.

What Type? Isolated or in superbubbles?

Galactic CR spectrum

$$dN/dE \propto E^{-2.75} \ (E<10^{15.5}\,\mathrm{eV})$$

Source spectrum

$$Q_{sour} \propto E^{-2.1\text{-}2.4}$$

DSA model $Q \propto E^{-2}$

Inconsistent ?

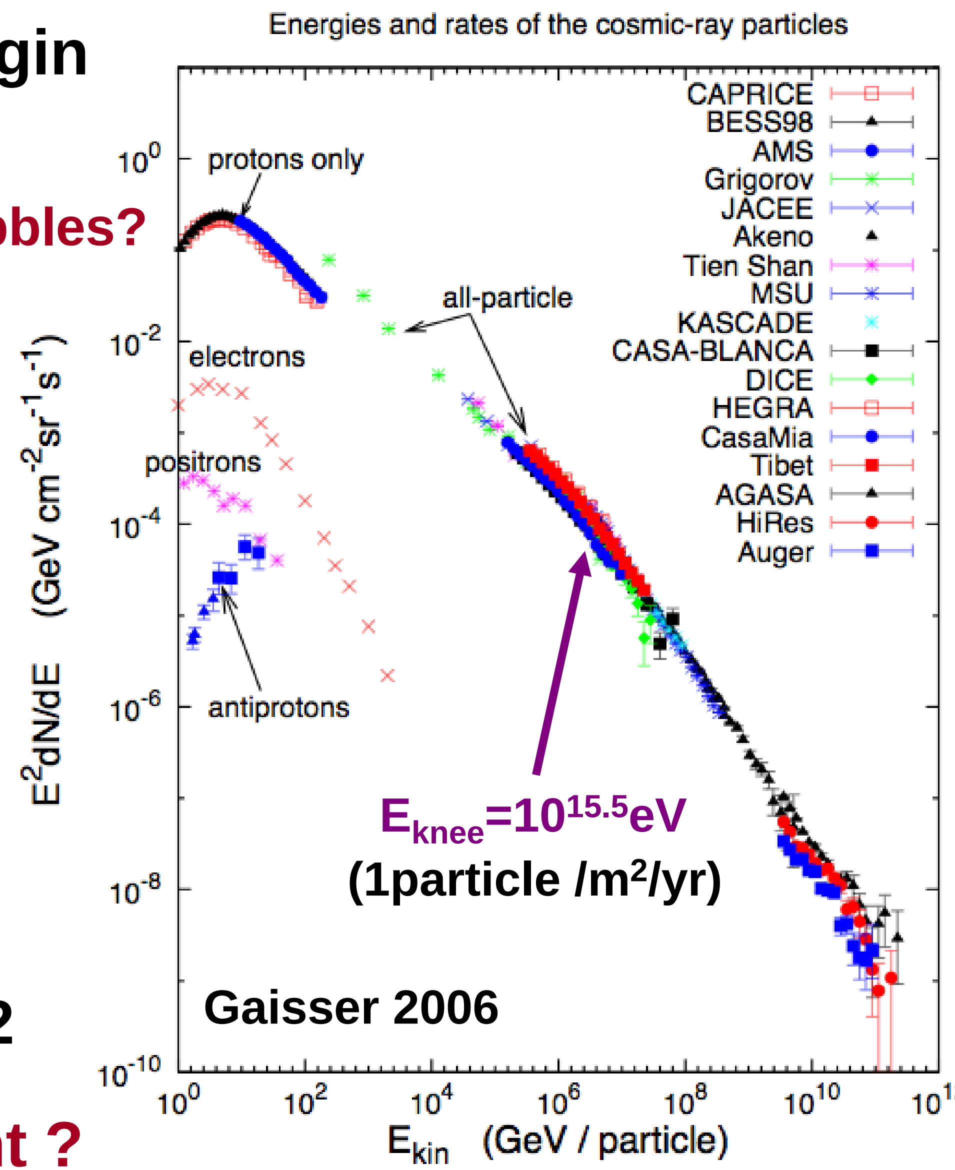

Observations of SNRs

s=2.2 for SN1006

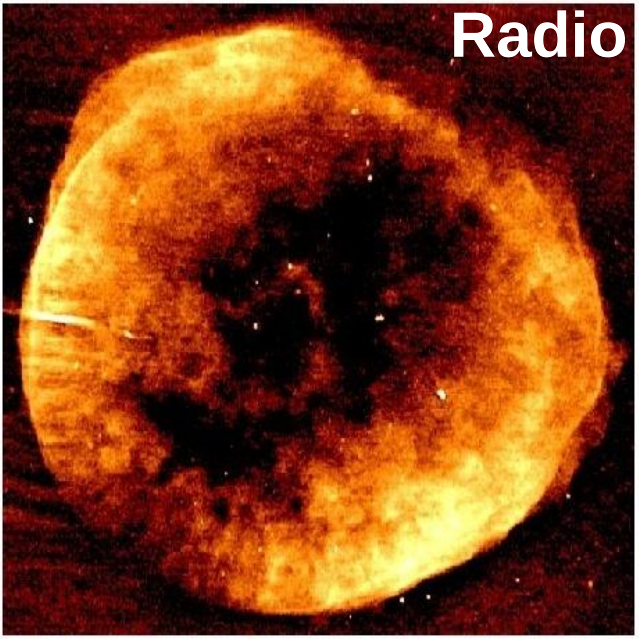

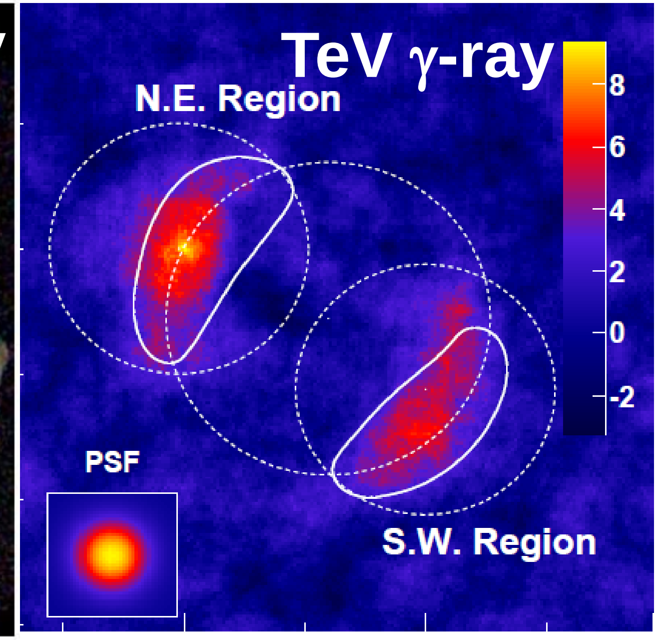

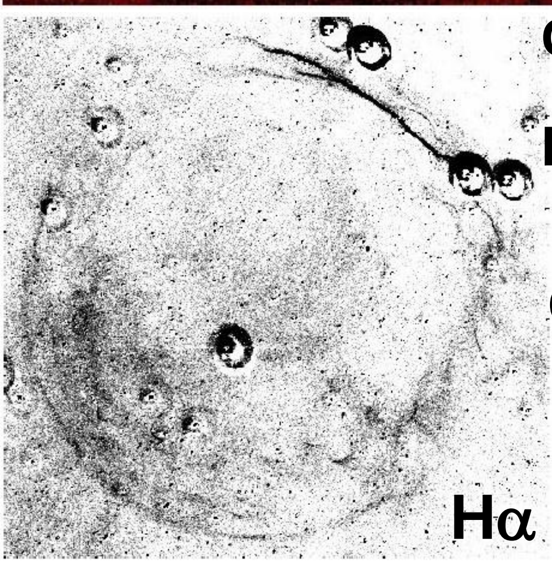

Cassam-Chenai et al. 2008

Acero et al. 2010

Radio : e^- acceleration up to GeV (~300 SNRs)

X ray : e^- acceleration up to TeV(~10 SNRs)

GeV-γ : p acceleration up to TeV(~10 SNRs)

TeV-γ : e^- or p accelerations up to 10TeV(~10SNRs)

$10^{15.5}$ eV?, 10^{50} erg/SN?, $K_{ep} = 10^{-2}$?, $dN/dE \propto E^{-2}$?

Diffusive Shock Acceleration(DSA)

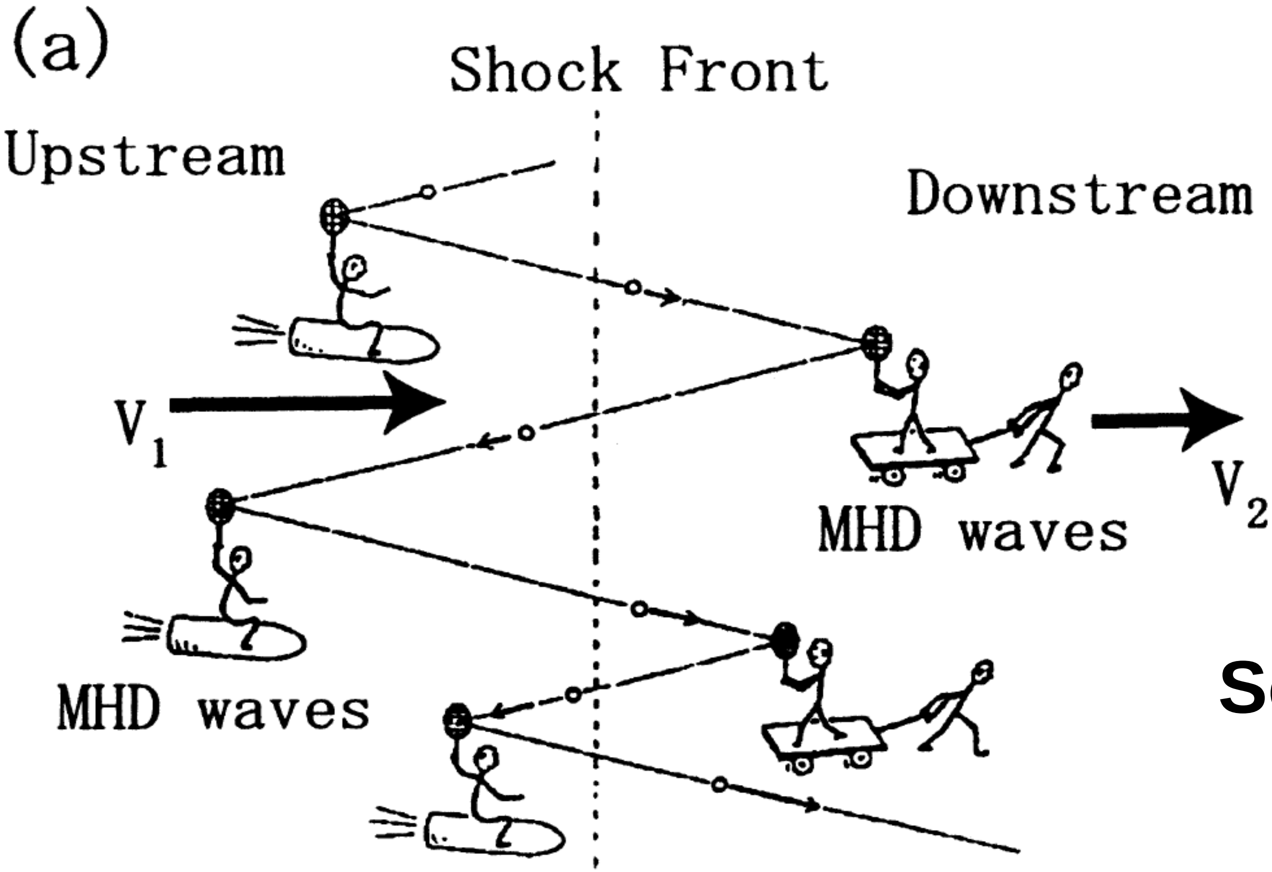

Scholer

$$dN/dE \propto E^{-s} \quad s = \frac{u_1/u_2 + 2}{u_1/u_2 - 1} = 2$$

Axford 1977, Krymsky 1977, Blandford&Ostriker 1978, Bell 1978

Effects on the spectral index

$dN/dE \propto E^{-s}$

Standard DSA theory	s = 2	Blandford & Ostriker, 1978
CR pressure	s < 2	Drury & Volk, 1981
Alfven wave drift	s > 2	Zirakashvili & Ptuskin, 2009
Escape of CR	s > 2	Ohira,Murase,Yamazaki, 2010
Anisotropy	s > 2	Bell et al., 2011
Neutral particles	s > 2	Ohira, 2012, Blasi et al. 2012
Sub diffusion	s > 2	Kirk et al., 1996
2nd order Fermi	s = ?	Fermi, 1949

Synchrotron radiation from accelerated e^-

Relativistic e^- + Magnetic field → Synchrotron radiation

$$dN_{e-}/dE \propto E^{-s} \rightarrow F_\nu \propto \nu^{-(s-1)/2}$$

$$\nu_{syn} = 0.29\,\gamma^2\,\Omega_{ce} / 2\pi \sim 5 \times 10^6\ \mathrm{Hz} \times E_{GeV}^2\ B_{\mu G}$$

1 GeV e^- + 300μG → ν_{syn} ~ 1.5 GHz

10 GeV e^- + 300μG → ν_{syn} ~ 150 GHz

100 GeV e^- + 3μG → ν_{syn} ~ 150 GHz

100 GeV e^- + 10μG → ν_{syn} ~ 500 GHz

Radio synchrotron is important for 1-100 GeV e^-

Spectral index in SNRs, s

Spectral index of radio synchrotron flux, $f_\nu \propto \nu^{-\alpha}$

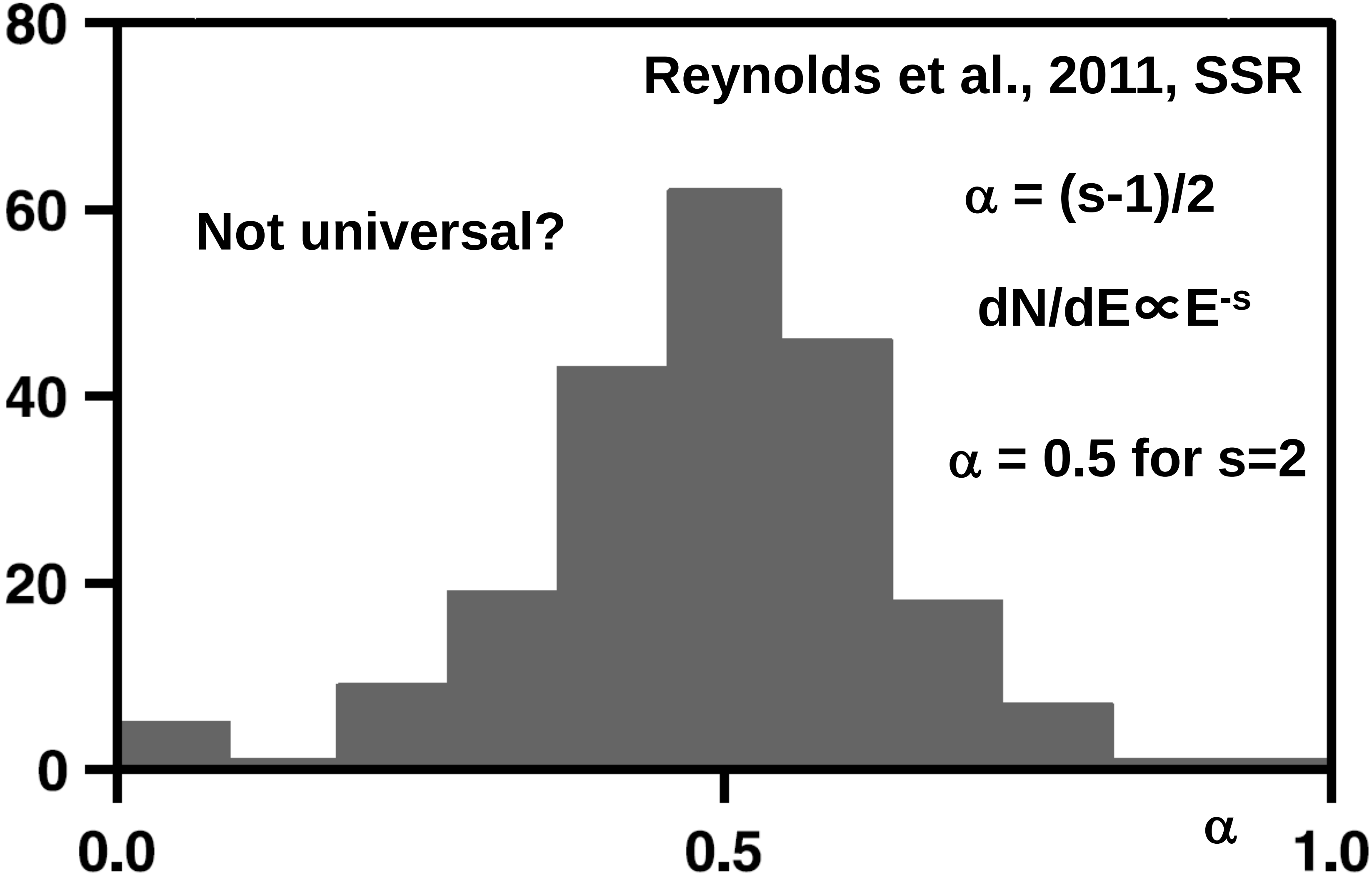

Young SNRs （SN1006）

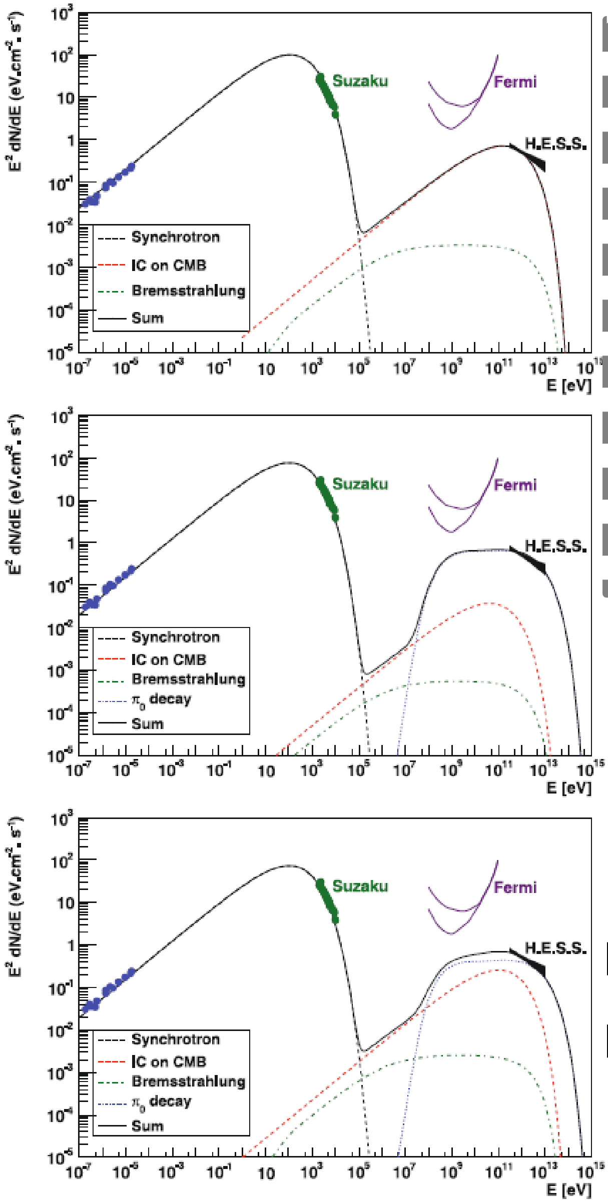

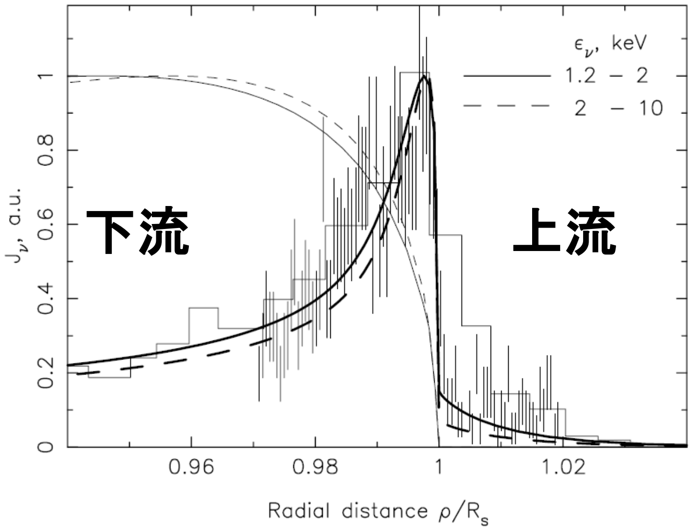

Berezhko et al.,2003, A&A, 412, L11

Radial profile of X-ray intensity

Thin width

Synchrotron cooling

→ B~100μG

Model	$E_{cut,e}$ [TeV]	$E_{cut,p}$ [TeV]	W_e [10^{47} erg]	W_p [10^{50} erg]	B [μG]
Leptonic	10	–	3.3	–	30
Hadronic	5	80	0.3	3.0	120
Mixed	8	100	1.4	2.0	45

Leptonic の問題: Small B、TeV specrum

Hadronicの問題: s_{proton} = 2.0 < $s_{electron}$ ~ 2.2

Which is better ?

Acero et al.,2010, A&A, 516, A62

CTA can identify the emission mechanism?

Young SNRs (RXJ1713)

Abdo et al., 2011, ApJ, 734, 28

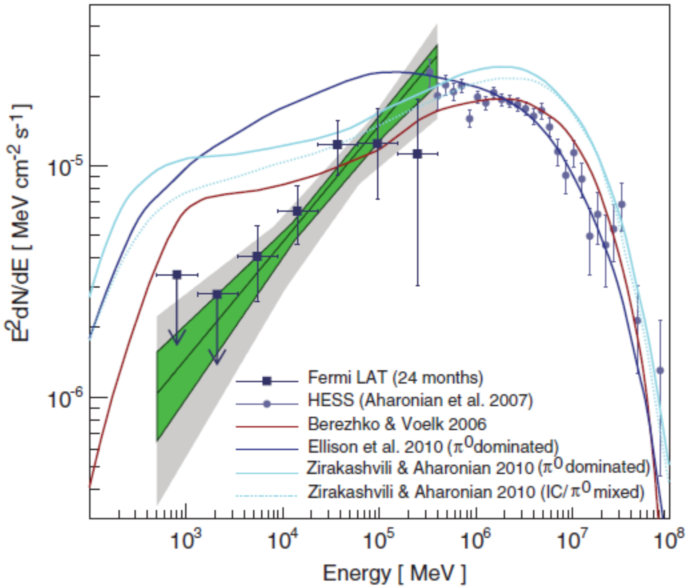

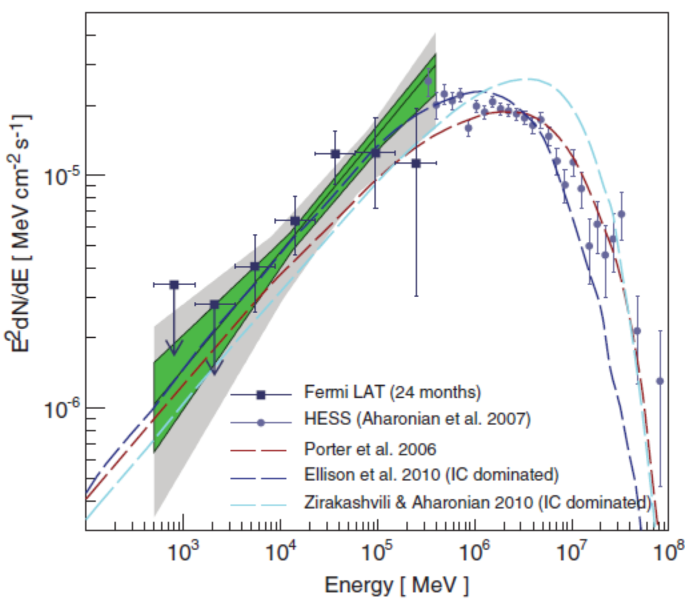

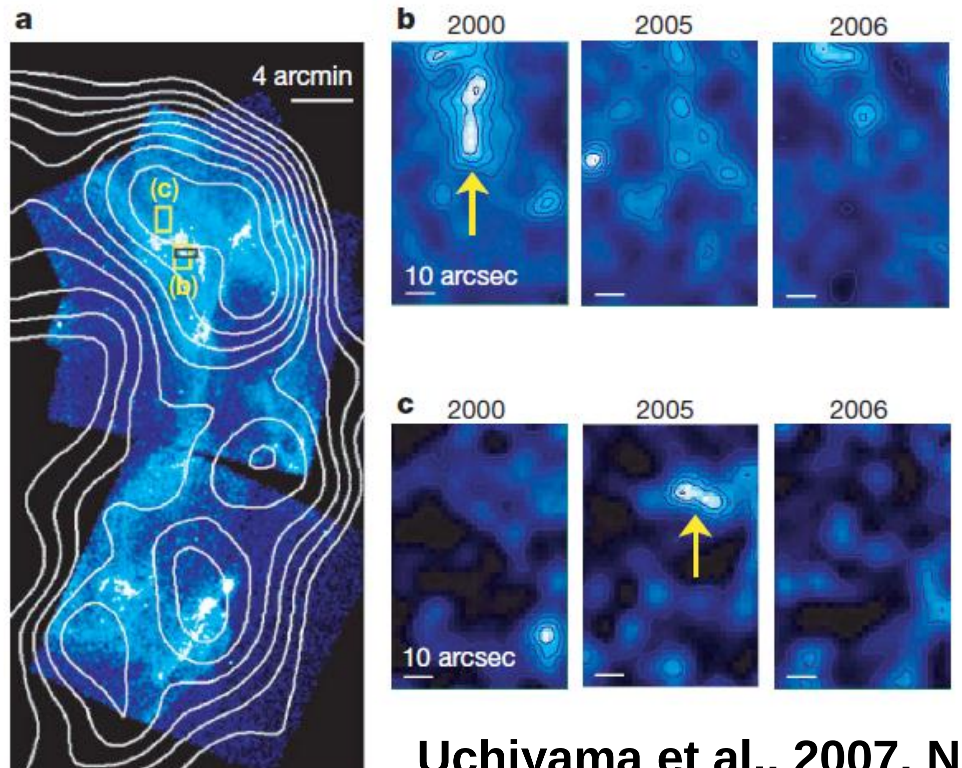

Uchiyama et al., 2007, Nature

~1yr time variability of x rays

→ t_{acc}, t_{cool} ~ 1yr

→ B~1mG B-field amplification?

Can CTA observe the time variability?

$W_p < 0.3 \times 10^{51} (n/0.1cm^3)^{-1}$erg

Young SNRs（Tycho）

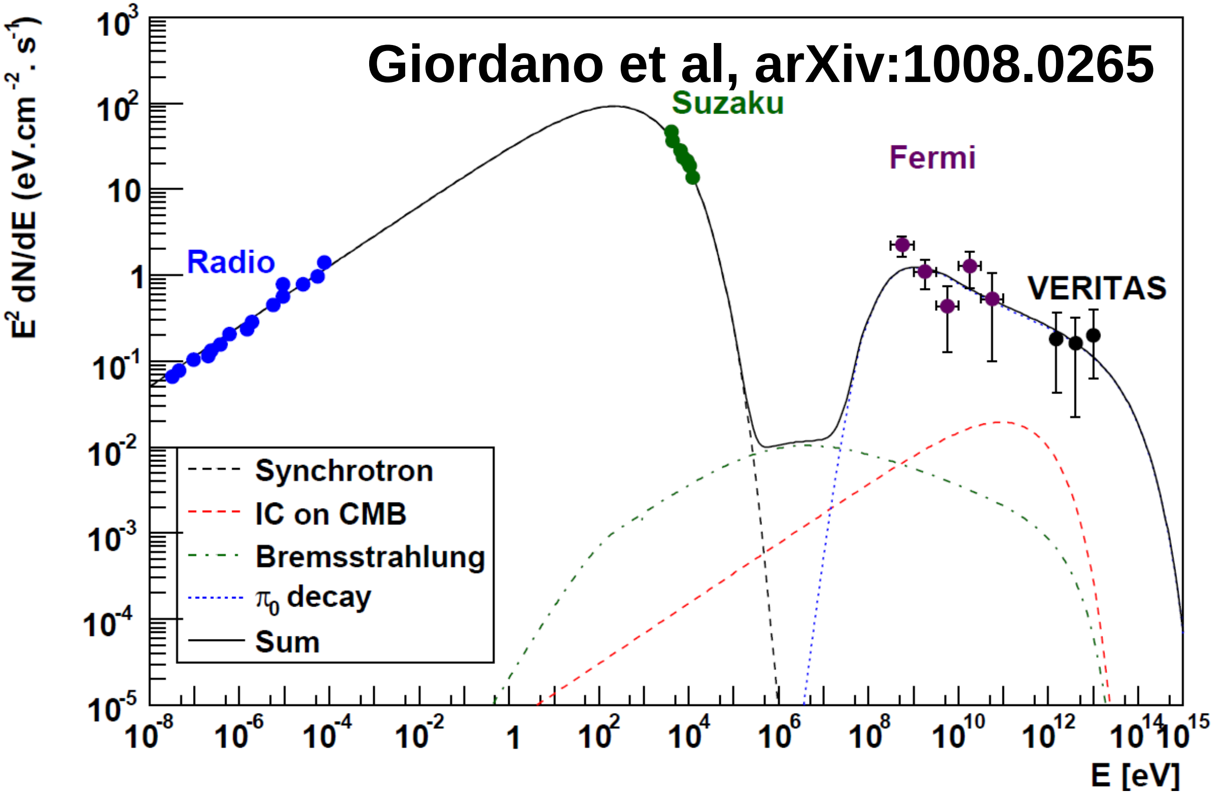

X-ray thin filaments
γ-ray flux
→ B~100μG

接触不連続面と
先進衝撃波の間が狭い

→ Compression ratio r > 4
s = (r+2)/(r-1)→ **s < 2**

$dN/dE \propto E^{-s}$

Case	D_{kpc} [kpc]	n_H [cm^{-3}]	E_{SN} [10^{51}erg]	$E_{p,tot}$ [10^{50}erg]	K_{ep} 10^{-4}	$E_{p,max}$ TeV
Far	3.50	0.24	2.0	1.50	4.5	540
Nearby	2.78	0.30	1.0	0.61	7.0	340

電波、ガンマ線スペクトルは **s = 2.3 < 2** （ Cas A も **s > 2** ）

加速された電子が少ない?

CTAによるTeV領域の高精度観測が必要

Young SNRs (Tycho, SN1006)

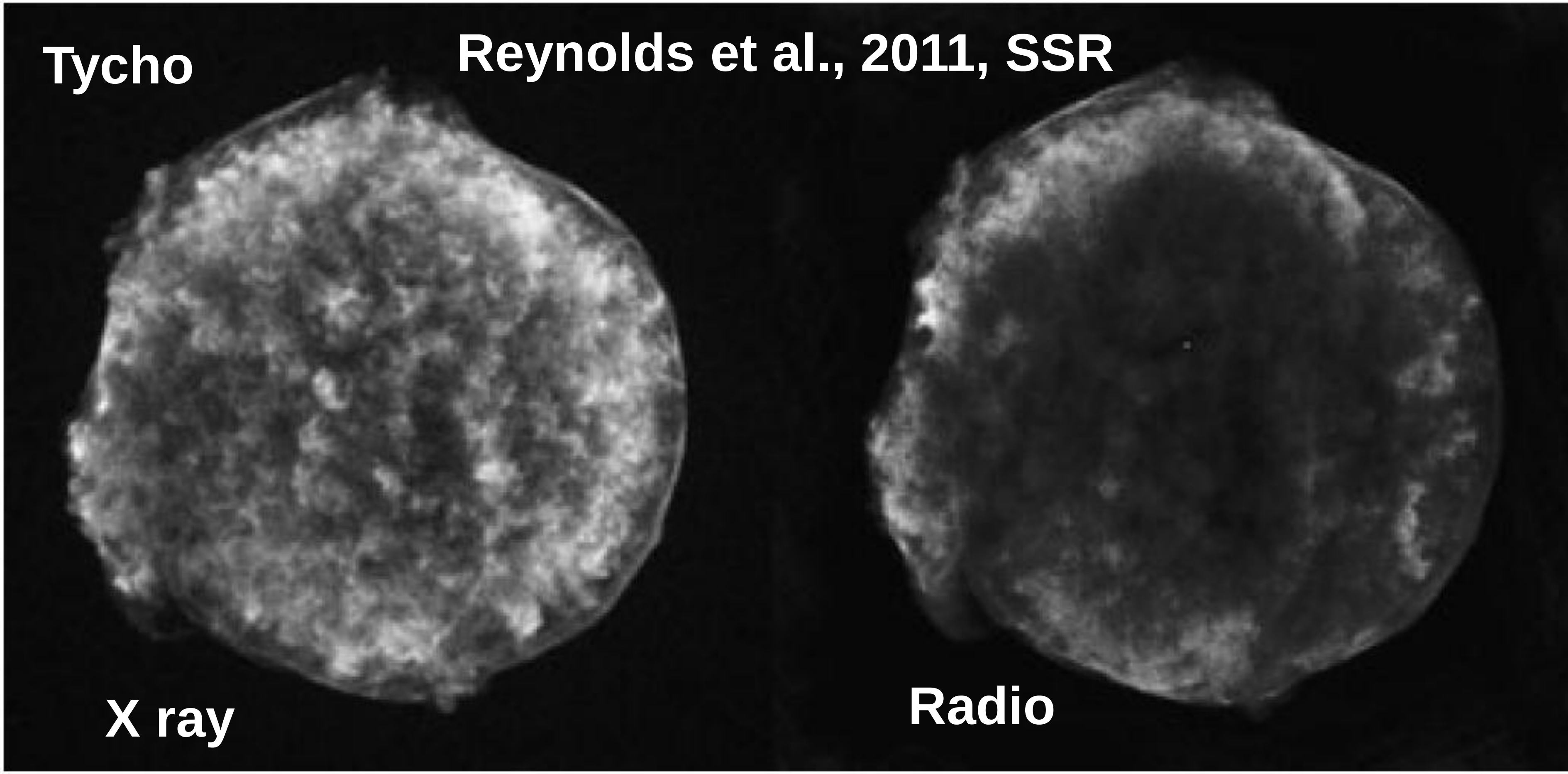

Thin filaments are observed not only in x ray but also in radio.

→ Magnetic damping? (M. Pohl et al., 2005, ApJL)

Where are electrons accelerated? Shock? Downstream? CD?

Young SNRs (Magnetic Field)

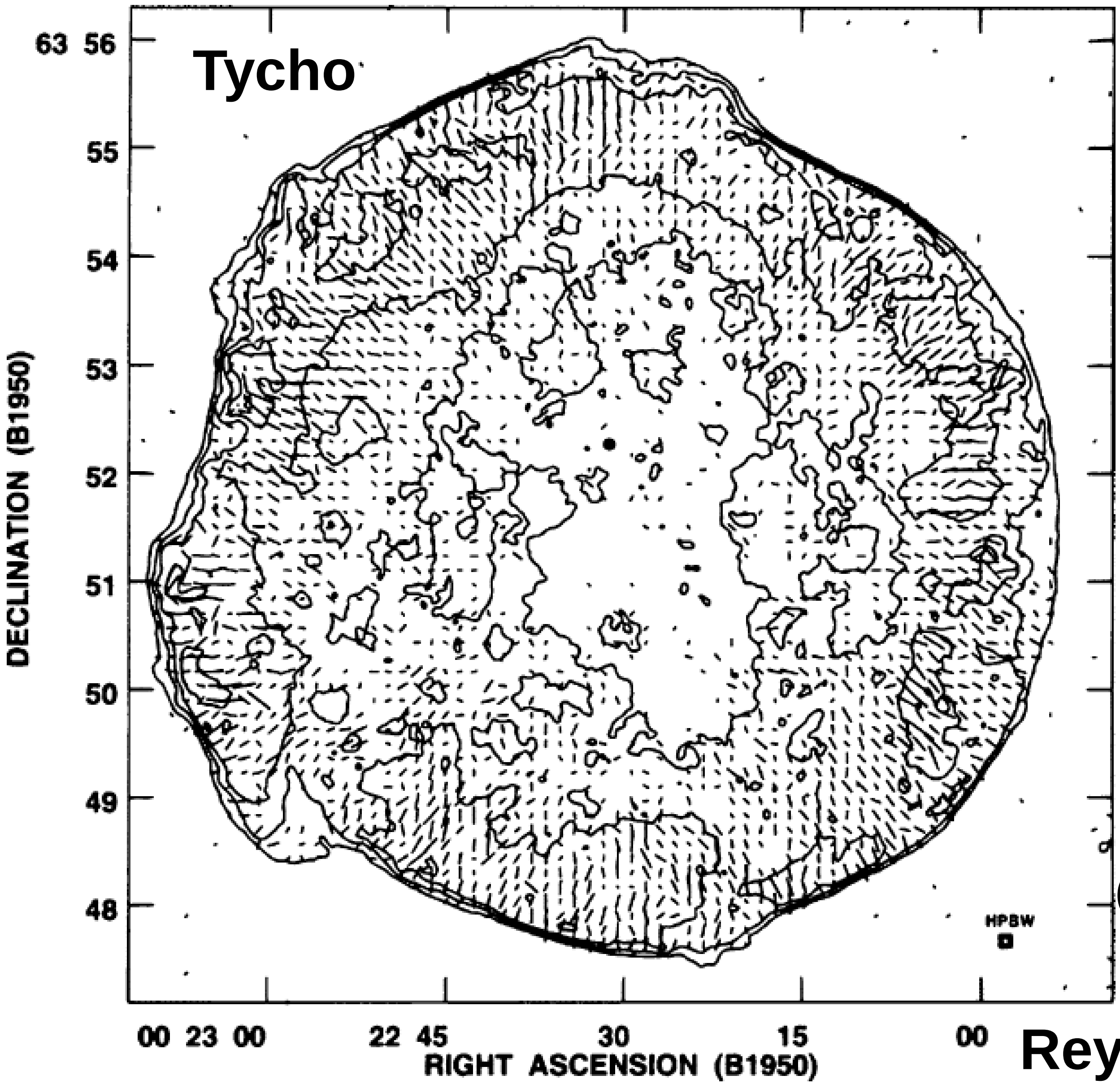

Everywhere, radial direction for young SNRs

(Dickel & Milne, 1976)

Why?

Rayleigh-Taylor instability?
(e.g. Schure, 2010)

Upstream density fluctuations?
(Zirakashvili&Ptuskin, 2008)

Reynoso et a., 1997, ApJ

Young SNRs (RCW86)

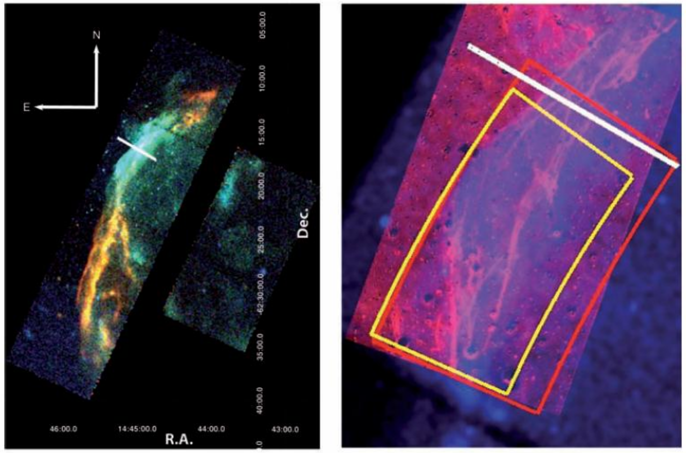

Fig. 1. (**Left**) The eastern rim of RCW 86, as observed in 2007 with Chandra. Red indicates the 0.5- to 1.0-keV band; green, the 1.0- to 1.95-keV band; and blue, the 1.95- to 6.0-keV band. The northern part has relatively more flux in the higher-energy bands, which is characteristic for synchrotron emission. (**Right**) Blue is the broadband keV Chandra image; red is the image as observed with the VLT through a narrow Hα filter. The regions (yellow and red) indicate where we measured the proper motion. In both panels, the location where we took the optical spectrum is indicated with a white line.

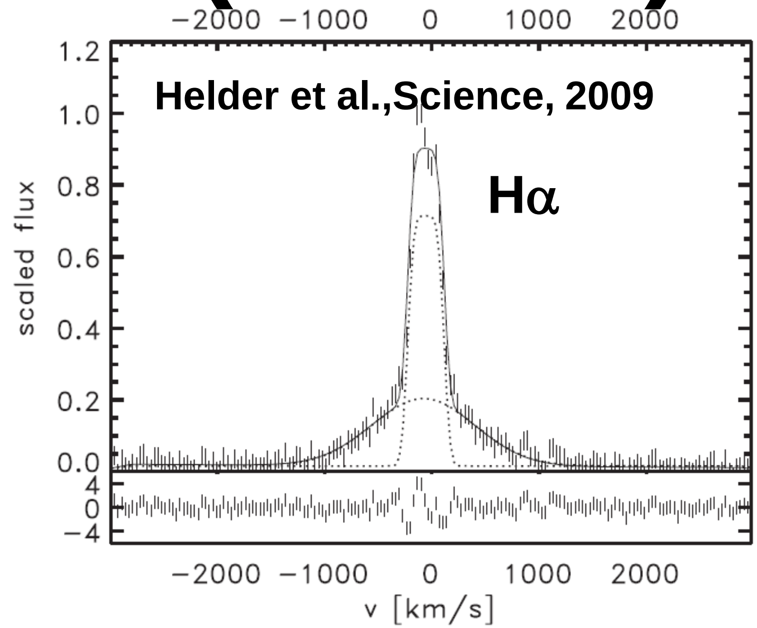

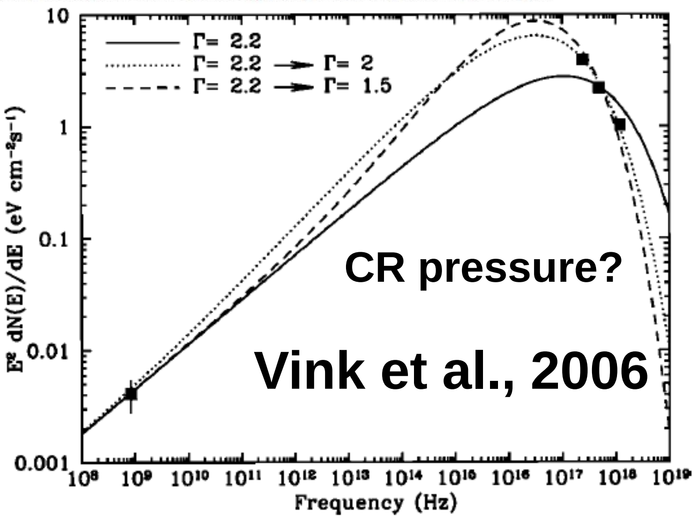

FIG. 4.—Broadband (νF_ν) spectrum of the NE region, with the 847 MHz flux density based on archival MOST data. The models consist of synchrotron radiation from a power law and concavely shaped electron energy distributions with exponential cutoffs at high energies, convolved with the synchrotron emission function (Ginzburg & Syrovatski 1965). The radio spectral index is fixed to $\alpha = -0.6$ (Caswell et al. 1975).

RCW86の場合、固有運動から衝撃波速度 u_{sh} ~6000±2800 km/s が観測されている。

$T_p = 3m_p u_{sh}^2/16 = 70$ keV

広い方の幅は、2.2 keVの温度に対応

→ CRがエネルギーを持ち去った？

狭い方の幅も広い → T_{up} ~ 30-100eV

→ CRが上流を加熱？

Effects of neutral hydrogen atoms
Ohira et al.(2009), Ohira & Takahara (2010), Ohira(2012)

Young SNRs（Cas A）

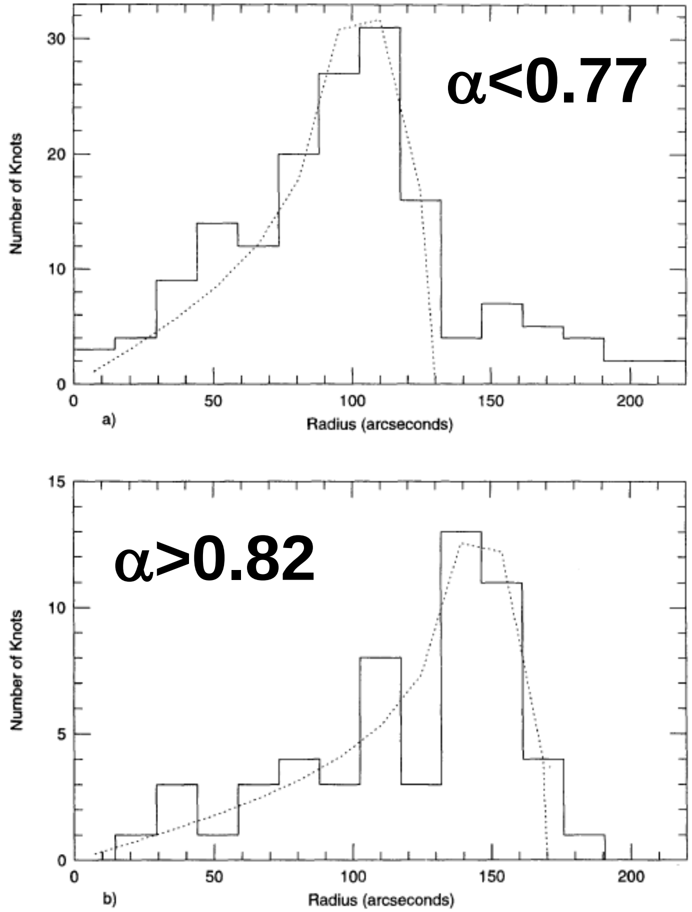

FIG. 4.—Histograms of projected radial position for (*a*) knots flatter th
$\alpha = 0.77$ and (*b*) knots steeper than $\alpha = 0.82$. Overlain in dotted lines,
comparison, are models of shells with uniform knot distributions and in
and outer radii (*a*) 95″–130″ and (*b*) 140″–170″.

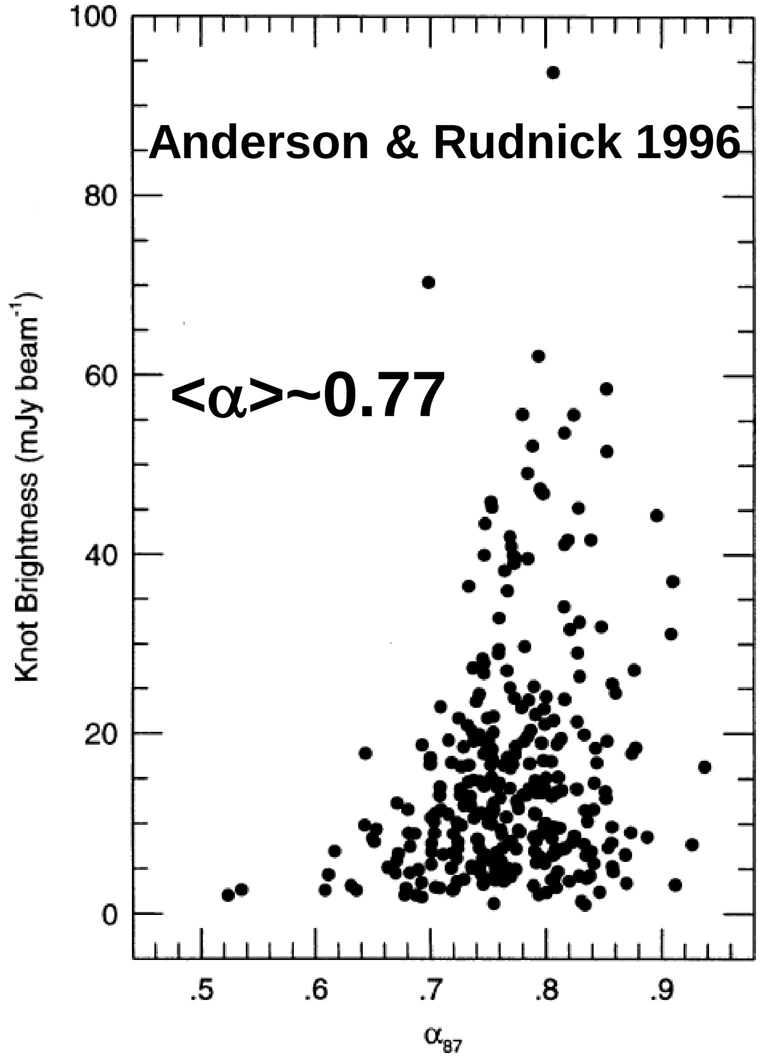

$f_{syn,\nu} \propto \nu^{-p}$

$dN/dE \propto E^{-s}$

$\alpha = (s-1)/2$

$\alpha = 0.77$

→ $s = 2.54$

Hard spectra at inner regions

Soft spectra at outer regions

Comparing the γ-ray index with radio index, we can identify the emission region.

Middle-aged（10^4yr）SNRs （W44）

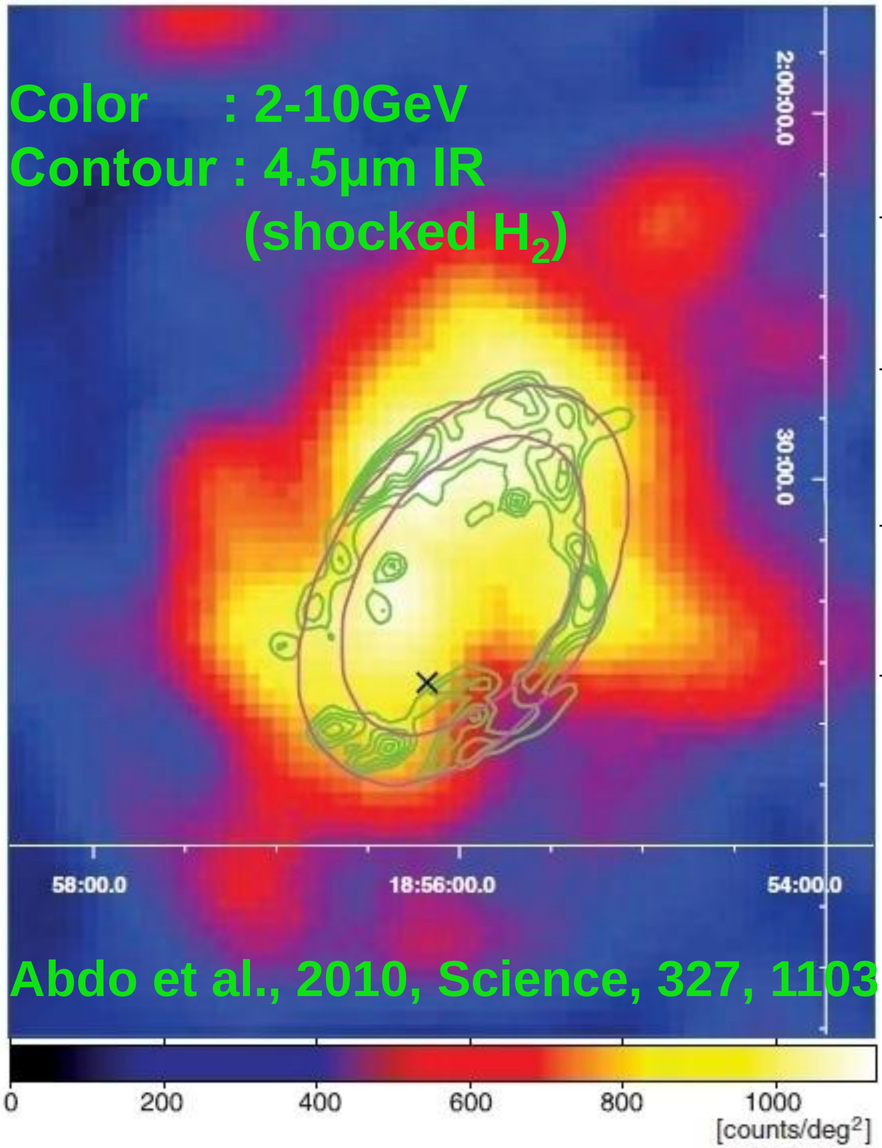

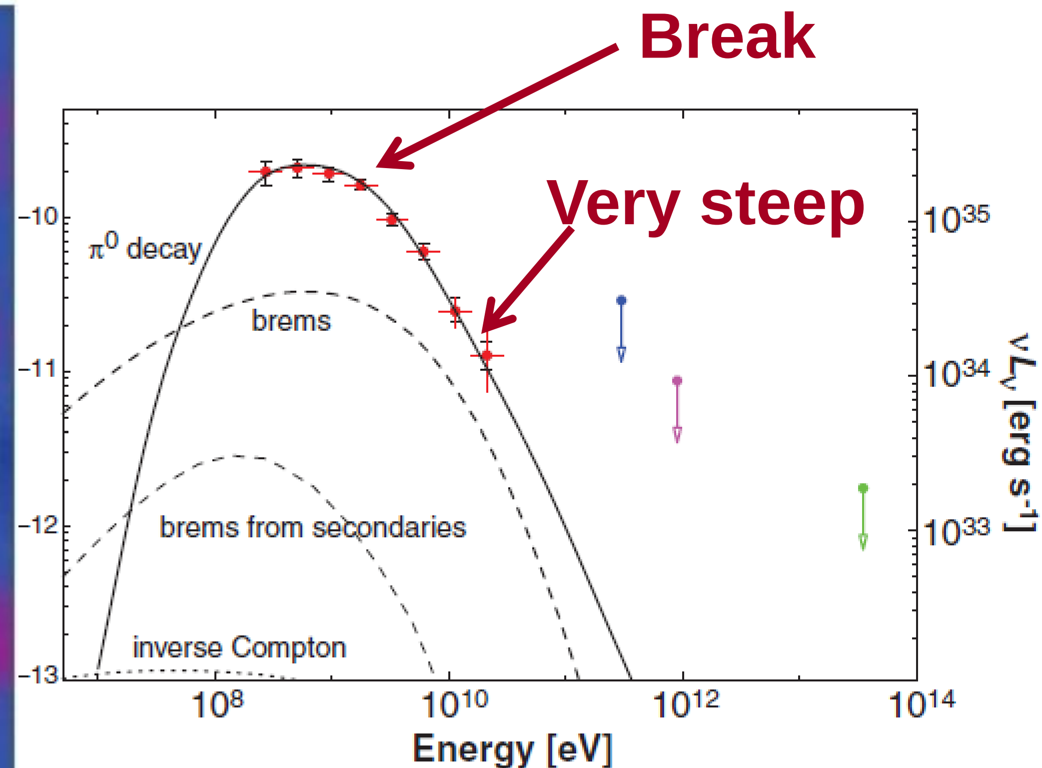

Broken power law
Very steep spectrum ($N(E) \propto E^{-3}$)

SNRs interacting with MC.

Escape of CRs from SNRs

Ohira,Murase,Yamazaki, MNRAS, 2011

Middle-aged（10^4yr） SNRs（Fermi SNRs）

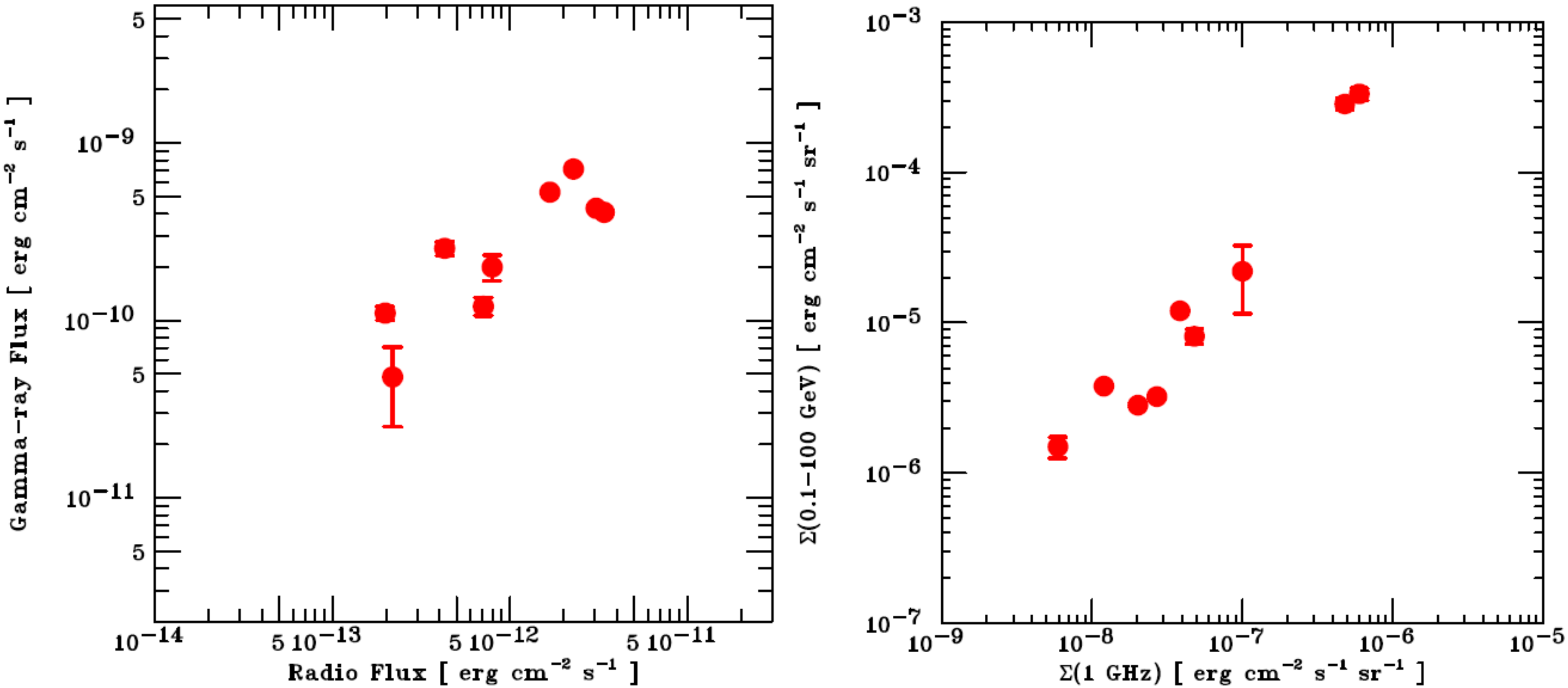

Figure 3: (Left) Radio flux (synchrotron) vs GeV γ-ray flux for MC-interacting SNRs. The γ-ray energy flux integrated over 0.1–100 GeV and the radio flux, νf_ν at 1 GHz, are shown. (Right) Mean surface brightness of the synchrotron radio emission and GeV γ-ray emission. The flux-flux plot is converted into this form using the solid angles of the radio remnants.

Uchiyama 2011

Radio vs TeV?

Middle-aged SNRs（Magnetic field）

Young SNRs

Old SNRs

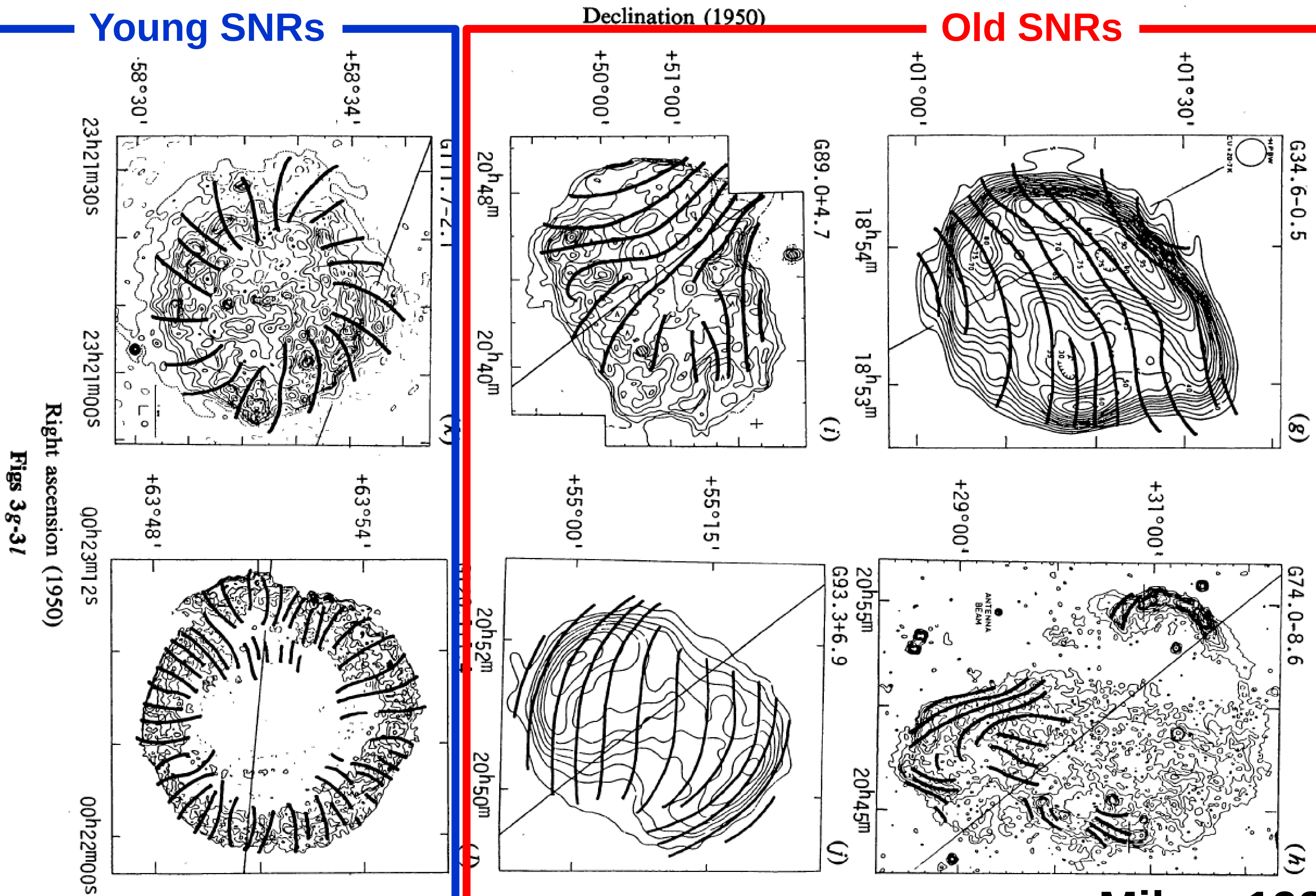

Milne, 1987

Middle-aged（10^4yr）SNRs （H_3^+）

Indriolo et al., 2010

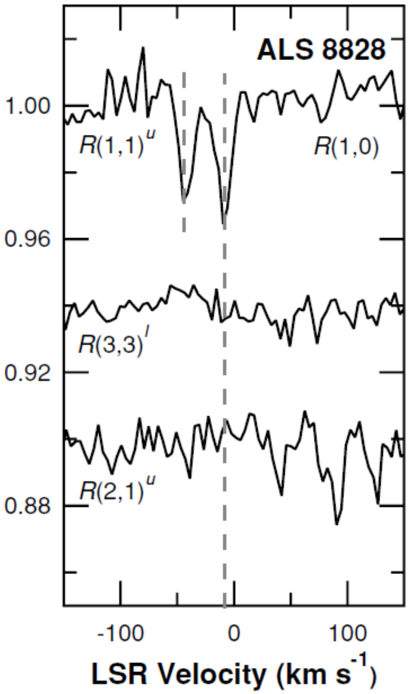

Tavani et al., 2010

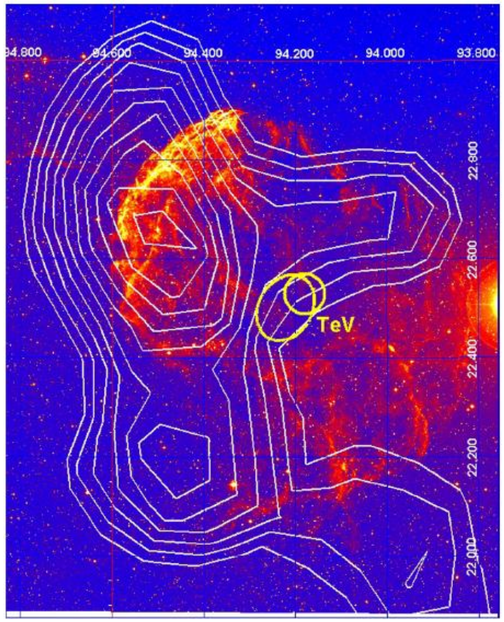

IC443 GeV-TeV γ ray

Ionization by Galactic CRs

Cosmic-Ray Ionization Rates (10^{-17} s^{-1})

Spectrum	ζ_2 $E_{\rm cut} = 2$ MeV (Diffuse)	ζ_2 $E_{\rm cut} = 10$ MeV (Dense)
Propagated[a]	1.4	1.3
Broken power law[a]	36	8.6
Carrot[a]	37	2.6
Hayakawa et al. (1961)	165	96
Spitzer & Tomasko (1968)	0.7	0.7
Nath & Biermann (1994)	260	34
Kneller et al. (2003)	1.3	1.0
Ip & Axford (1985)[b]	3.6	2.7
Herbst & Cuppen (2006)	0.9	0.9
Observational inferences	~40[c]	~3[d]

Indriolo et al., 2009

$$\sigma_{\rm ion} = 2\pi(0.285)\frac{e^4}{m_ec^2{\rm Ry}}\frac{Z^2}{\beta^2}\left[\ln\frac{2m_ec^2\beta^2}{0.048(1-\beta^2){\rm Ry}} - \beta^2\right] = 1.23\times10^{-20}\frac{Z^2}{\beta^2}\left(6.2+\log_{10}\frac{\beta^2}{1-\beta^2} - 0.43\beta^2\right)\ {\rm cm}^2$$

Absorption by H_3^+ → CR ionization rate

CR + H_2 → CR + H_2^+ + e^-

H_2 + H_2^+ → H_3^+ + H

H_3^+ + e^- → H_2 + H or H + H + H

Ionization = recombination

$\zeta_2 n(H_2) = k_e n_e n(H_3^+)$

→ $\zeta_2 \sim 10^{-15}$ s^{-1} > 10^{-16} s^{-1}

Very Young SNRs (SN1987A)

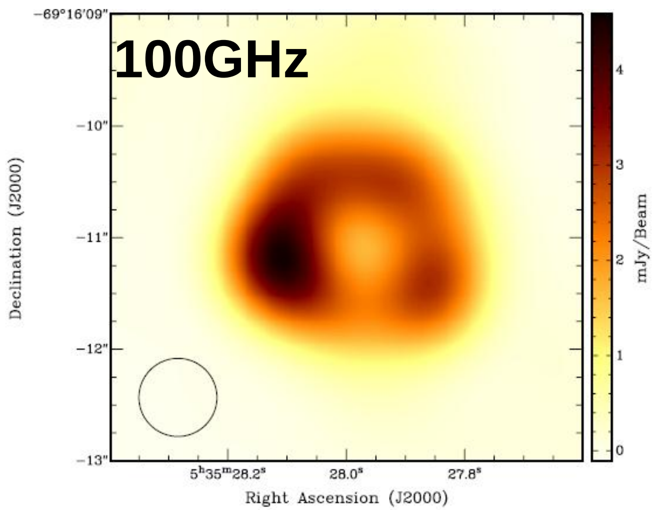

Fig. 1. Diffraction-limited Stokes-I continuum image of SNR 1987A at 3 mm from observations made on 2011 June 30, July 1 and August 2. The image is restored to a 0.″7 circular beam (plotted in the lower left corner). The off-source rms noise is ≈0.5 mJy $beam^{-1}$.

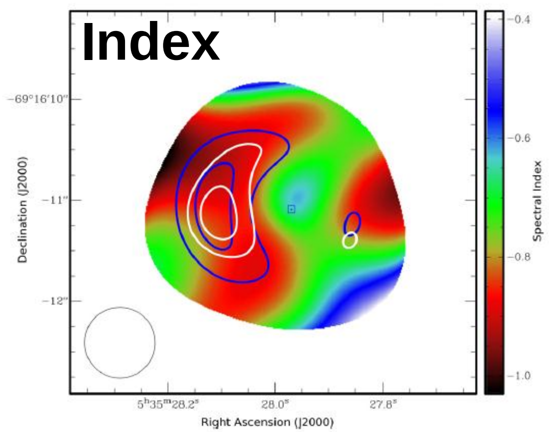

Fig. 5. 3-mm – 3-cm spectral index image. The spectral index α is defined as $S_\nu \propto \nu^\alpha$ and was determined from the ratio of the 3-cm image from observations performed on 2011 January 25 (Ng. et al., in prep.) and the 3-mm image from observations around July 2011. Both images were restored on a 0.″7 circular beam and centred on the VLBI position of SN 1987A determined by Reynolds et al. (1995) (blue square). The images are overlaid with contours representing the 70% and 90% flux density levels (white: 3 mm; blue: 3 cm).

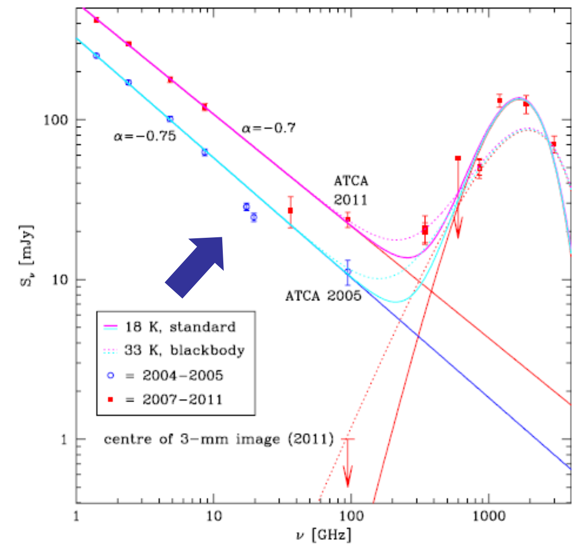

Fig. 2. IR-radio SED of SNR 1987A with data from Matsuura et al. (2011), Lakićević et al. (2011, 2012), Zanardo et al. (2010), and this work. Power laws are fitted to $\lambda > 30$ cm, and two different models for dust emission are plotted (cf. Lakićević et al. 2012). The upper limit of 1 mJy is plotted for any emission in the centre of the 2011 image at 3 mm in addition to that extrapolated from the synchrotron power-law.

Lakicevic et al. 2012

$t_{age} \sim 25$ yr , $dN/dE \propto E^{-2.4}$

The spectral index is not uniform.

Broken power law spectrum

$$t_{cool,syn} \sim 1.5 \times 10^{10}\ \mathrm{yr} \times B_{\mu G}^{-2}\, E_{GeV}^{-1}$$

$$\sim 10\ \mathrm{yr} \times B_{100mG}^{-3/2}\, \nu_{syn,10GHz}^{-1/2}$$

Cooling break?

B field amplification

Very Young SNRs (SN1993J)

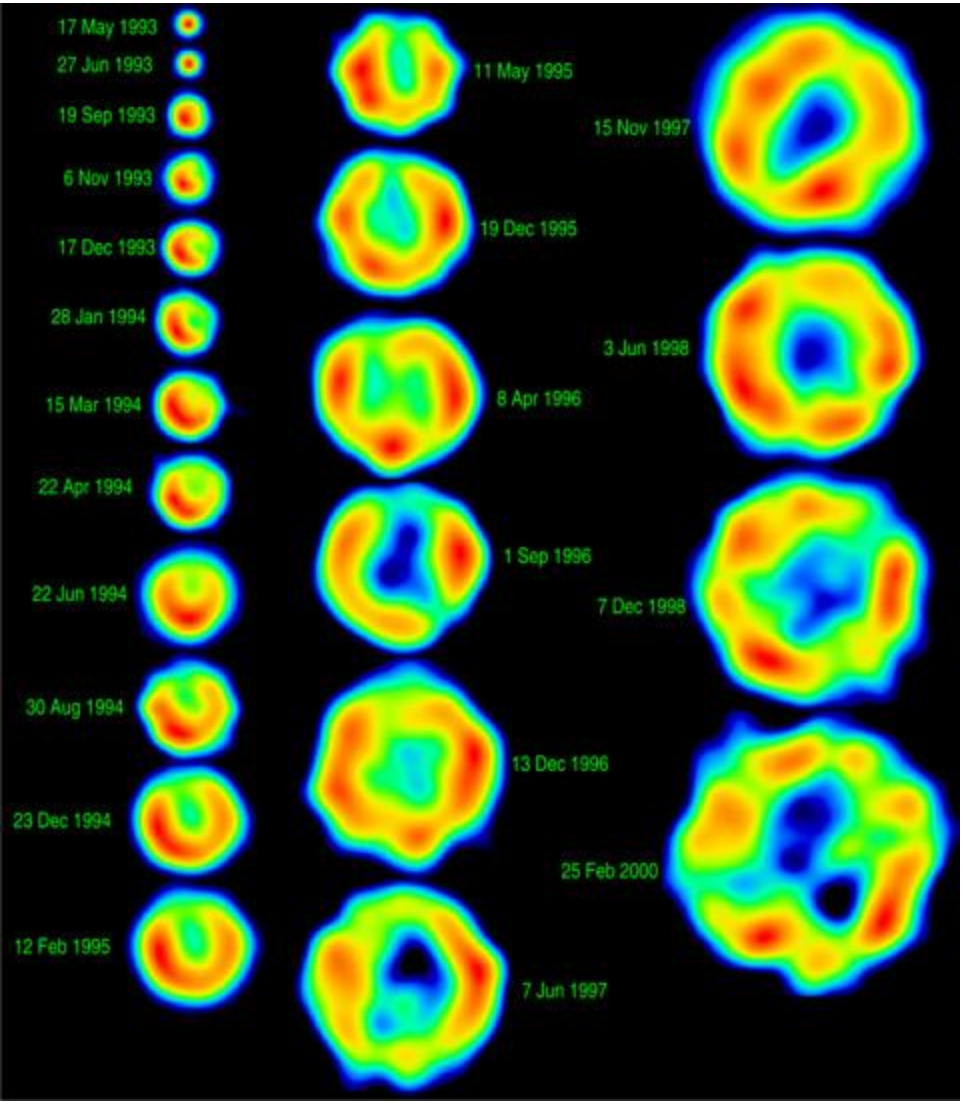

Image courtesy of NRAO/AUI and N. Bartel, M. Bietenholz, M. Rupen, et al.

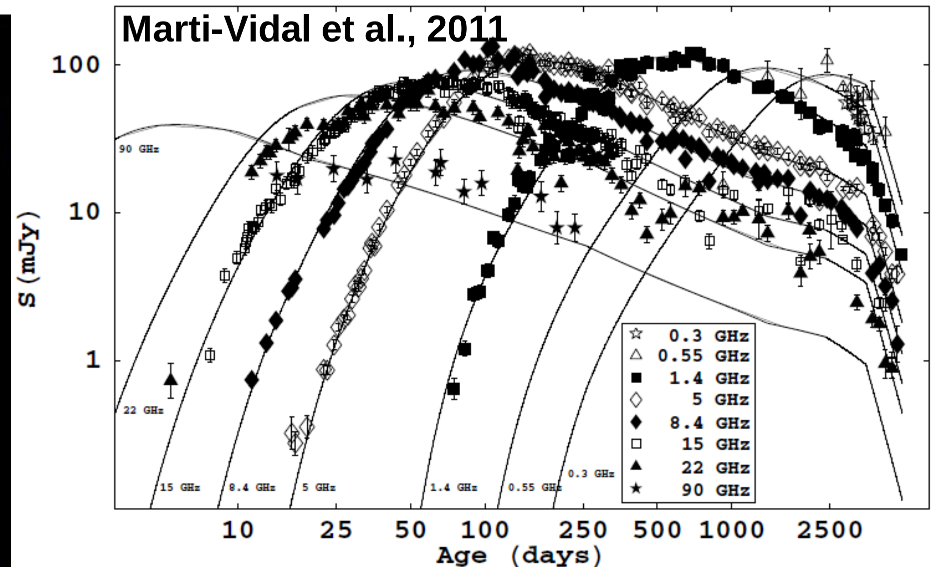

t_{age} ~ 20yr , $dN/dE \propto E^{-2.55}$

γ-ray flux of extragalacitc SNRs

$$E^2 \frac{dF_\gamma}{dE} \sim \frac{U_{CR} n \sigma_{pp} c}{4\pi d^2}$$

$$\sim \frac{0.1 \times \frac{4\pi}{3} R^3 \times \frac{1}{2}\rho v^2 \times n\sigma_{pp} c}{4\pi d^2}$$

$$\sim 1.7 \times 10^{-13}\, erg/s/cm^2 \times n_2{}^2 v_9{}^5 t_{10yr}{}^3 / d_{Mpc}{}^2$$

Very Young PWNe? (SN1986J)

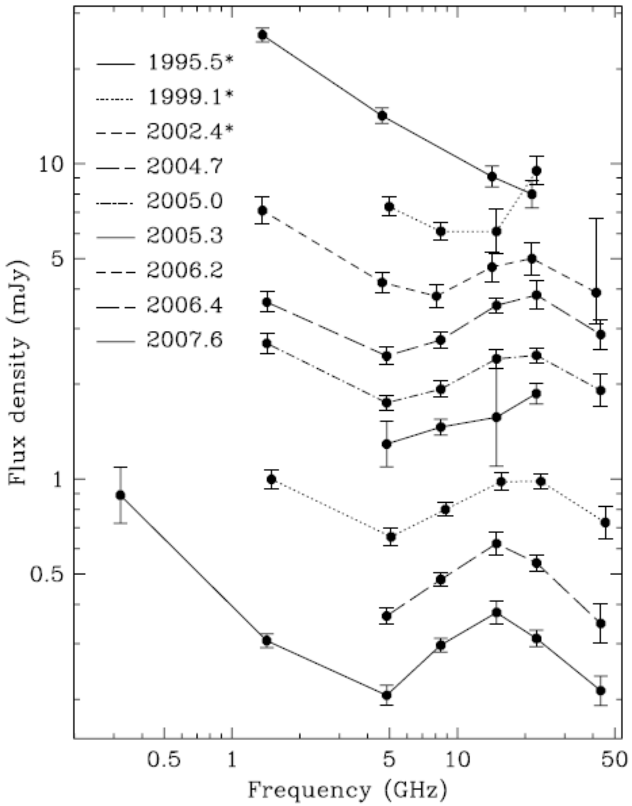

Figure 2. Evolving radio spectrum of SN 1986J, as determined from VLA observations. Each curve shows the radio spectrum at the epoch indicated at left, with the earliest spectrum at the top. The flux-density scale on the left axis is relevant directly for the first three curves from the top (1995.5, 1999.1, and 2002.4), whose epochs are marked with an asterisk. The other curves are shifted logarithmically progressively downward for better visibility, so that the spectral shape is preserved even though the flux density scale is not. The curves are shifted by the following factors: 2004.7 by 0.80, 2005.0 by 0.60, 2005.3 by 0.50, 2006.2 by 0.25, 2006.4 by 0.15, and 2007.6 by 0.10. The uncertainties are estimated standard errors, including statistical and systematic contributions. The data include both our own and re-reduced archival data (see Table 2).

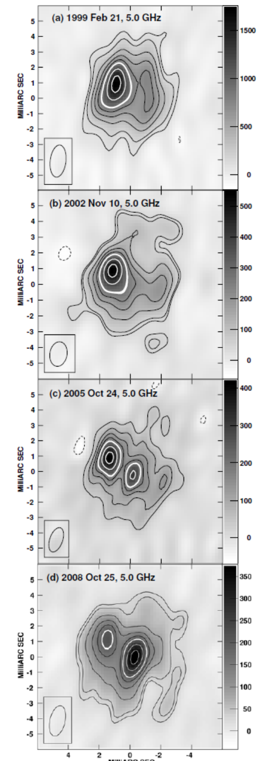

Figure 3. Sequence of VLBI images of SN 1986J at 5 GHz, showing its evolution over the last decade. In each panel, the coordinate system is centered on the estimated position of the center of the shell ($02^h22^m31^s.321457$, $42°19'57''.25951$; see the text). The contours are in percent of the peak brightness, with negative ones being dotted. Each panel has contours at 10%, 20%, 30%, 40%, **50%**, 70%, and 90%, with the 50% one being emphasized and the lowest white one. The lowest contours, given for each panel below, are 3 times the rms background brightness. The FWHM size of the convolving beam is indicated at lower left in each panel. North is up and east is to the left. (a) 1999 February 21, 5 GHz. The peak brightness was 1720 μJy beam^{-1}, the lowest contour 5.5%, the rms background brightness 31 μJy beam^{-1}, and the convolving beam 2.09 × 1.02 mas at p.a. −7°. (b) 2002 November 10, 5 GHz. The peak brightness was 543 μJy beam^{-1}, the lowest contour 7.6%, the rms background brightness 14 μJy beam^{-1}, and the convolving beam 1.57 × 1.12 mas at p.a. −10°. The visibility data were tapered slightly in u to increase signal to noise and produce a somewhat less elongated beam. (c) 2005 October 24, 5.0 GHz. The peak brightness was 414 μJy beam^{-1}, the lowest contour 9.3%, the rms background brightness 13 μJy beam^{-1}, and the convolving beam 1.65 × 0.83 mas at p.a. −20°. (d) 2008 October 25, 5.0 GHz. The peak brightness was 388 μJy beam^{-1}, the lowest contour 7%, the rms background brightness 9.0 μJy beam^{-1}, and the convolving beam was 2.02 × 0.98 mas at p.a. −13°.

(An animation of this figure is available in the online journal.)

γ-ray flux of extragalacitc PWNe

$$E^2 \frac{dF_\gamma}{dE} < \frac{L_{spin}}{4\pi d^2}$$

$$\sim 10^{-11}\, erg/s/cm^2 \times \left(\frac{L_{spin}}{10^{39} erg}\right)\left(\frac{d}{1Mpc}\right)^{-2}$$

If radiative efficiency > 1%, extragalactic PWNe can be observed by CTA!

Bietenholz et al.,2010

http://iopscience.iop.org/0004-637X/712/2/1057/fulltext/

Summary

Standard DSA predicts $dN/dE \propto E^{-2}$

Observations show $s \neq 2$. $dN/dE \propto E^{-s}$

CTAによるスペクトルの決定は理論への制限に重要！

TeVガンマ線の放射領域がSNR内で決められないとき、
indexによって決めることが可能。Index の決定精度が重要！

Magnetic field is strongly amplified around SNR shocks

IC成分のスペクトルとFluxの決定が重要

Magnetic field directions are radial for young SNRs
and tangential for old SNRs

About 50 very young SNRs (Radio Supernovae)have been observed.

CTA will be able to observe extragalactic SNRs and PWNe